

Transit time enhanced bandwidth in nanostructured terahertz emitters

S. C. Corzo-Garcia, M. Alfaro and E. Castro-Camus

Received: date / Accepted: date

Abstract Monte-Carlo simulations are used to show that the transit time in ~ 100 nm gap photoconductive emitters of terahertz radiation is short enough to produce broad-bandwidth pulses. Furthermore, with these calculations we demonstrate that nanostructured contacts remove the need for low-temperature-grown or ion-implanted materials for broad-band terahertz devices.

Keywords photoconductive · nano · terahertz · THz · spectroscopy

Since their introduction in 1983,[1] terahertz (THz) photoconductive devices have been the subject of intensive study for over three decades.[2–5] Ion-implanted semiconductors have shown promising characteristics for the fabrication of such devices,[6, 7] yet, low-temperature-grown GaAs (LT-GaAs) remains the material of choice for the fabrication of THz photoconductive switches.[8] Although enormous progress has been achieved in the low-temperature growth process,[9] the reproducibility of optoelectronic parameters, namely carrier lifetime and mobility, is still difficult. In addition, the introduction of defects in the crystalline lattice of GaAs produced by the low-temperature growth or the ion-implantation process imply a trade-off between high mobility and short carrier lifetime.[10] Therefore the possibility of using standard semi-insulating GaAs or other standard high mobility semiconductors could significantly reduce the cost and open the possibility for mass production of THz photoconductive devices. Previous studies have shown that it is possible to use the transit time to replace the need for LT-GaAs in photoconductive detectors.[11] In this article we demonstrate that the transit time between contacts with a separation of ~ 100 nm is short enough to obtain emission

S. C. Corzo-Garcia
Centro de Investigaciones en Óptica A.C., Loma del Bosque 115, Lomas del Campestre,
León, Guanajuato 37150, México
Tel.: +52 (477) 441-42-00
Fax: +52 (477) 441-42-09
E-mail: enrique@cio.mx

bandwidths comparable or better to those obtained from LT-GaAs based emitters with ~ 250 fs carrier lifetimes, even for substrates with long-lived carriers (~ 10 ns).

The study we present is based on a semi-classical Monte-Carlo simulation of carrier dynamics in semiconductors.[12] The semiconductor we simulated is GaAs and all the parameters in the simulation were set accordingly.[13] In our Monte-Carlo model an ultra-short laser pulse of 60 fs of duration and central wavelength of 800 nm is simulated. The carriers generated by such a pulse move classically in 1 fs steps in a three-dimensional box ($30\mu\text{m} \times 30\mu\text{m} \times 10\mu\text{m}$ or $10\mu\text{m} \times 10\mu\text{m} \times 10\mu\text{m}$). At every time step, scattering probabilities for each particle are calculated considering the following mechanisms: carrier-carrier, LO-phonon mediated inter-valley ($\Gamma \rightleftharpoons L \rightleftharpoons X$), acoustic phonon, neutral and ionized impurities. Computer generated quasi-random numbers are used to determine if each particle is scattered, its scattering angle and energy change. Afterwards, the charge density is calculated over a fine grid of the three-dimensional box ($300 \times 200 \times 200$ divisions). Using the carrier density, the Poisson equation is numerically solved in order to obtain the potential and electric field which is used, at its time, to calculate the force acting on every particle for the next time step. This process is iterated over 5000 time steps. Carriers are removed exponentially with time constant τ in order to simulate trapping and/or recombination. This Monte Carlo approach provides a very detailed representation of the actual carrier dynamics in the semiconductor used for the photoconductive emitter. The simulation calculates the emitted THz electric field using the far field approximation

$$E_{\text{THz}} \propto \frac{\partial \mathbf{J}}{\partial t}. \quad (1)$$

More details on the simulation can be found in Refs. [12–14].

The boundary conditions for the Poisson solution are Neumann conditions for the bottom and the four sides of the box. The front face is divided into three parts (see Fig. 1e). The potential is fixed to 0 on the first part (grounded cathode), V_b is set on the third part which is the bias voltage (anode) that can be changed by the user and Neumann condition is set for the intermediate part (gap). This way the contacts and gap between contacts of the photoconductive emitter are simulated. The size of the gap can also be controlled by the user.

Using the simulation described above, we modeled the carrier dynamics in photoconductive emitters with short (250 fs typical of LT-GaAs) and long (10 ns typical of SI-GaAs) carrier lifetimes, both with small (100 nm) and large ($10\mu\text{m}$) gaps. The resulting terahertz pulses and their Fourier transforms are shown in Fig. 1. From the graph it is clear that the carrier lifetime has an enormous effect on the duration of the pulse produced from the large gap antenna. The short carrier lifetime results in a shorter THz pulse and therefore on a broader spectrum. Interestingly the waveform, and spectra, for both carrier lifetimes in the small gap antenna show negligible differences, these two pulses show relatively short durations and broad spectra when compared to the larger gap simulations.

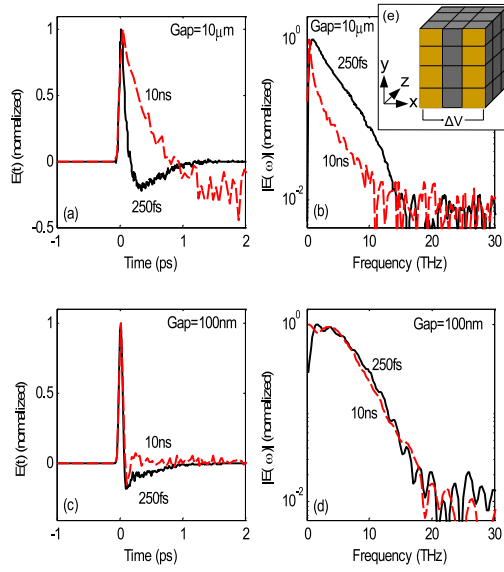


Fig. 1 (Color online) (a) Simulated electric field waveform of a terahertz pulse generated by a 10 μm gap photoconductive antenna on substrates with 250 fs and 10 ns carrier lifetimes respectively. (b) Shows the amplitude spectra of the waveforms shown in (a). (c) Simulated waveform of a terahertz pulse generated by a 100 nm gap photoconductive antenna on substrates with 250 fs and 10 ns carrier lifetimes respectively. (d) Shows the amplitude spectra of the waveforms in (c). (e) Shows a schematic representation of the geometry and boundary conditions used for the Monte Carlo simulation.

In order to understand these differences we plot the charge density for various times after photoexcitation for emitters with long carrier lifetime. The colormaps in panels a and b of Fig. 2 show the charge density for a large and small gap emitter respectively at the moment of photoexcitation showing no significant differences. The subsequent panels in Fig. 2 correspond to 50 fs, 100 fs and 200 fs after photoexcitation where remarkable differences arise. The dipole formation, responsible for the terahertz emission, in the small gap antenna occurs within the first ~ 100 fs reaching an almost steady state while the dipole is still forming in the 10 μm gap device after 200 fs. This difference can be attributed to the shorter distance that carriers have to travel in the small gap emitter. This suggests that transit time might be the dominating factor that determines the duration of the terahertz transients in small gap emitters.

Of course, the carrier transit time between contacts is determined by both the separation between such contacts and speed of carriers. In a simplistic approximation the speed is proportional to the applied electric field. Therefore, if transit time is the main factor that determines the terahertz pulse duration and spectral width in the 100 nm gap device, it should show a significant dependence on the applied field. A series of simulations for both gap sizes were

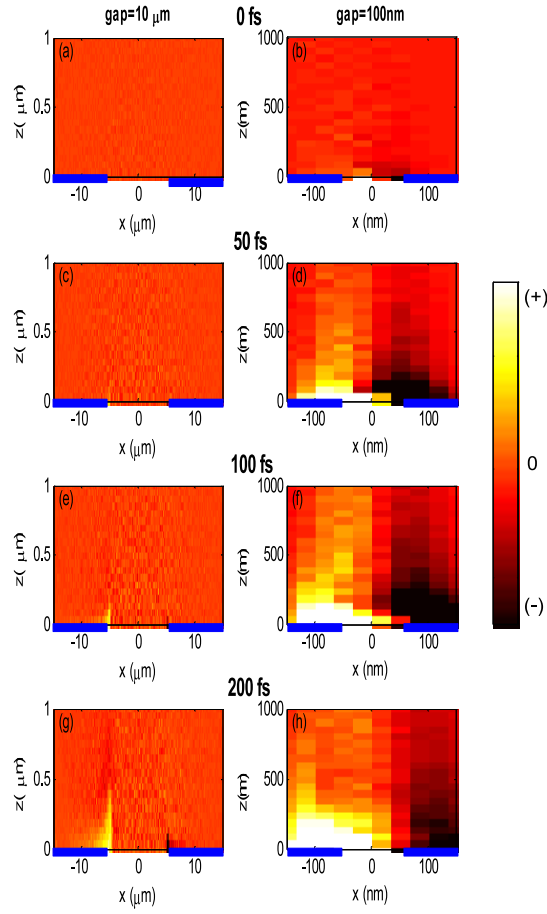


Fig. 2 (Color online) Carrier density for a $10\ \mu\text{m}$ (a) and $100\ \text{nm}$ (b) gap photoconductive emitter at the moment of the optical pulse arrival. The contacts are indicated by a thick (blue) line. The following panels (c) and (d), (e) and (f), (g) and (h) show analogous plots for times 50 fs, 100 fs and 200 fs after the photoexcitation pulse. The simulations correspond to an applied bias electric field of $30\ \text{kV cm}^{-1}$.

run for different bias voltages, such that bias electric fields from $10\ \text{kV cm}^{-1}$ to $40\ \text{kV cm}^{-1}$ were applied across the two gap sizes. The plot shown in Fig. 3 contains 4 curves of the full-width-at-half-maximum (FWHM) of the resulting spectra. The FWHM gives a quantitative measure of the bandwidth. Notice that a large gap with a long carrier lifetime produces a FWHM of only $\sim 1\ \text{THz}$, the same large gap with a short carrier lifetime produces $\sim 3\ \text{THz}$ FWHM, both with no significant electric field dependence. The small gap structure produces a bandwidth of $\sim 6.5\ \text{THz}$ for the short carrier lifetime with little dependence on the electric field. Interestingly, the small gap structure with long carrier life-

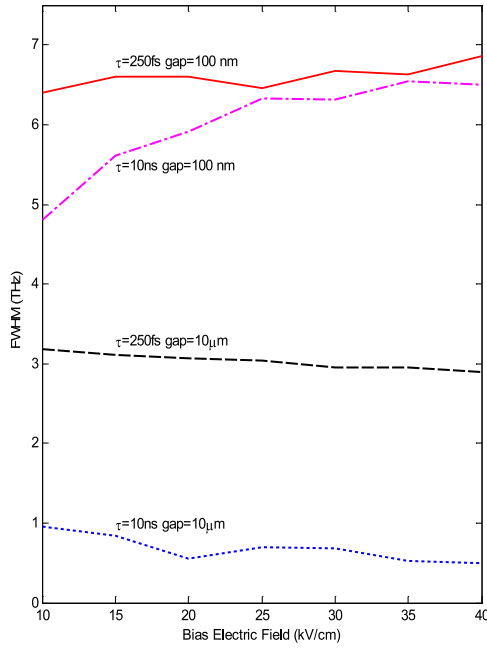


Fig. 3 (Color online) Spectral bandwidth (full-width-at-half-maximum) of terahertz pulses simulated for 10 μm and 100 nm gaps with 250 fs and 10 ns carrier lifetimes.

time generates spectra with a FWHM that changes from ~ 5 THz to ~ 6.2 THz for bias voltages between 10 kV cm^{-1} and 25 kV cm^{-1} , for higher bias voltages the FWHM dependence seems to be less important and its value approaches that of the small gap and short carrier lifetime device.

The results of this simulation demonstrate that broad bandwidth terahertz pulses (spectra $\text{FWHM} > 5$ THz) can be generated from sub-micron gap photoconductive emitters made on long carrier lifetime (~ 10 ns) semiconductors. According to the simulation, this bandwidth can be even better than that of standard micrometric gap antennas fabricated on short carrier lifetime (~ 250 fs) substrates such as LT-GaAs. The simulation indicates that this broadening can be attributed to the shorter transit time of carriers between the photoconductive emitter contacts.

The possibility of fabricating broad bandwidth emitters on long carrier lifetime semiconductors is rather attractive. Firstly, the cost and reproducibility of low-temperature-grown and ion-implanted semiconductors is inadequate for the implementation of terahertz time-domain spectroscopy on real-world applications. Secondly, the higher mobility of long carrier lifetime semiconductors can result in higher terahertz electric fields, and therefore better signal-to-noise

performance of the emitters. In addition plasmon-enhanced coupling of the optical radiation combined with three-dimensional nano-patterned contacts have demonstrated extraordinary optical-to-terahertz efficiency.[15] Therefore our results in combination with these other recently published studies suggest that photoconductive emitters with nanostructured contacts could become a standard low-cost and high-performance terahertz technology in the future.

1 Acknowledgements

The authors would like to thank CONACyT (México) [Grant no. 131931]. S.C. Corzo-Garcia wants to acknowledge a scholarship from CONACyT [No. 327556]

References

1. D.H. Auston, P.R. Smith, *Appl. Phys. Lett.* **43**, 631 (1983)
2. Y.C. Shen, P.C. Upadhyaya, H.E. Beere, E.H. Linfield, A.G. Davies, I.S. Gregory, C. Baker, W.R. Tribe, M.J. Evans, *Appl. Phys. Lett.* **85**, 164 (2004)
3. H. Makabe, Y. Hirota, M. Tani, M. Hangyo, *Opt. Express* **15**, 11650 (2007)
4. N. Vieweg, M. Mikulics, M. Scheller, K. Ezdi, R. Wilk, H.W. Hübers, M. Koch, *Opt. Express* **16**, 19695 (2008)
5. C. Berry, N. Wang, M. Hashemi, M. Unlu, M. Jarrahi, *Nature communications* **4**, 1622 (2013)
6. T.A. Liu, M. Tani, M. Nakajima, M. Hangyo, C.L. Pan, *Appl. Phys. Lett.* **83**, 1322 (2003)
7. B. Salem, D. Morris, V. Aimez, J. Beerens, J. Beauvais, D. Houde, *J. Phys.-Condes. Matter* **17**, 7327 (2005)
8. Y.C. Shen, P.C. Upadhyaya, E.H. Linfield, H.E. Beere, A.G. Davies, *Appl. Phys. Lett.* **83**, 3117 (2003)
9. I.S. Gregory, C. Baker, W.R. Tribe, M.J. Evans, H.E. Beere, E.H. Linfield, A.G. Davies, M. Missous, *Appl. Phys. Lett.* **83**, 4199 (2003)
10. E. Castro-Camus, L. Fu, J. Lloyd-Hughes, H.H. Tan, C. Jagadish, M.B. Johnston, *J. Appl. Phys.* **104**, 053113 (2008)
11. B. Heshmat, H. Pahlevaninezhad, Y. Pang, M. Masnadi-Shirazi, R. Burton Lewis, T. Tiedje, R. Gordon, T.E. Darcie, *Nano Letters* **12**(12), 6255 (2012). DOI 10.1021/nl303314a. URL <http://pubs.acs.org/doi/abs/10.1021/nl303314a>
12. E. Castro-Camus, J. Lloyd-Hughes, M.B. Johnston, *Phys. Rev. B* **71**, 195301 (2005)
13. M.B. Johnston, D.M. Whittaker, A. Corchia, A.G. Davies, E.H. Linfield, *Phys. Rev. B* **65**, 165301 (2002)
14. J. Lloyd-Hughes, E. Castro-Camus, M.B. Johnston, *Solid State Commun.* **136**, 595 (2005)
15. C.W.B.M.J. S.-H. Yang, M. R. Hashemi, *IEEE Transactions on Terahertz Science and Technology* **4** (2014)